21st IAHR International Symposium on Ice
"Ice Research for a Sustainable Environment"
Dalian, China, June 11 to 15, 2012

Convective Mixing by Solar Radiation under Lake Ice

Georgiy Kirillin[1*], William Rizk[1] and Matti Leppäranta[2]
1. Department of Ecohydrology, Leibniz-Institute of Freshwater Ecology and Inland Fisheries, Berlin,Germany
2. Department of Physics, University of Helsinki, Helsinki, Finland
[*]kirillin@igb-berlin.de

Convection caused by solar radiation is the main driver for mixing under ice in spring and is the most energetic process in ice-covered lakes. It affects ice melting rate and has important ecological implications, in particular, by providing the vertical transport mechanism for non-motile plankton species. In temperate lakes, convection depends strongly on the diurnal radiation cycle. We present the first data on the convective shear microstructure with the daytime variations resolved. In addition, for the first time the convection characteristics were achieved for the period immediately preceding the ice break-up, when fieldwork from the ice surface is not possible. The results validate the shear microstructure method for the under-ice convection in the absence of mean flow and provide the direct quantitative estimations of the convective mixing intensity. We outline the range of the convective variability within a day and its dependence on the amount of solar radiation penetrating the ice cover. The appropriate mixed layer scaling is discussed.

1. Introduction

In frozen lakes without a snow cover, a significant amount of solar radiation penetrates through the ice into the water column. Heating of the upper water column and subsequent sinking of warmer and heavier waters produce convection, which takes place at the background of stable density stratification, so that the convectively mixed layer of uniform temperature/density gets thicker with time and penetrates into the stably stratified fluid below. Convective mixing due to solar heating is the most energetic transport process in ice-covered lakes and dominates the circulation during the melting season.

A distinctive feature of convection under lake ice is the absence of mean flow and the corresponding shear mixing that makes ice-covered lakes to an outstanding “natural laboratory” for investigation of purely convective flow. This fact, together with relatively small spatial scales as compared to atmospheric or oceanic flows allowing relatively easy-to-perform measurements, has drawn the attention of geophysicists. Farmer (1975) performed first systematic observations of radiatively-driven convection in a deep ice-covered freshwater Lake Babine and presented an analysis of the convective mixing efficiency. Mironov et al. (2002) summarized observations from various lakes and presented a comprehensive review of previous studies on this topic. They also elaborated an appropriate scaling for the convection in frames of the kinetic energy budget integrated over the convective mixing layer and constructed a one-dimensional mixed layer model.

Apart from being a rare natural example of free convection without mean flow, radiation-driven convection is of extreme importance to primary production in ice-covered lakes. Vertical convective motions help non-motile plankton species to stay in the upper photic layer and be supplied by the nutrients from the deeper waters (Hobbie 1973; Matthews und Heaney 1987; Jewson u. a. 2009). Therefore, much attention has been paid to estimation of the vertical convective velocities and of the convectively mixed layer depth subject to external factors, primarily to the radiation flux under ice.

Convection produces a mixed layer of homogeneous temperature bounded by two stably stratified layers from above and from below (Fig. 1). In a relatively thin surface layer between the mixed layer and the ice surface, temperature increases from the freezing point at the ice-water interface to the value characteristic of the bulk of the convectively mixed layer. A quiescent fluid beneath the convective layer is usually stably stratified due to heat loss to the ice and heat inflow from the sediment during the period preceding the convection. Heating by the solar radiation continuously increases the temperature of the mixed layer and its thickness by entrainment of the water from the stably stratified layer below. If mixing achieves the lake bottom, warming of the mixed layer accelerates, since no energy is spent for the entrainment. Therefore, the depth differences between shallow and deep parts of lakes are able to produce lateral temperature gradients and initiate a density-driven circulation (Farmer 1975; Bengtsson 1986). Other factors affecting the intensity of the convective mixing under ice are ice an water transparency, which affect amount of radiation under ice and its distribution over the water column. Diurnal as well as synoptic variations in incoming solar radiation over the lake surface also cause significant variations in the convection strength.

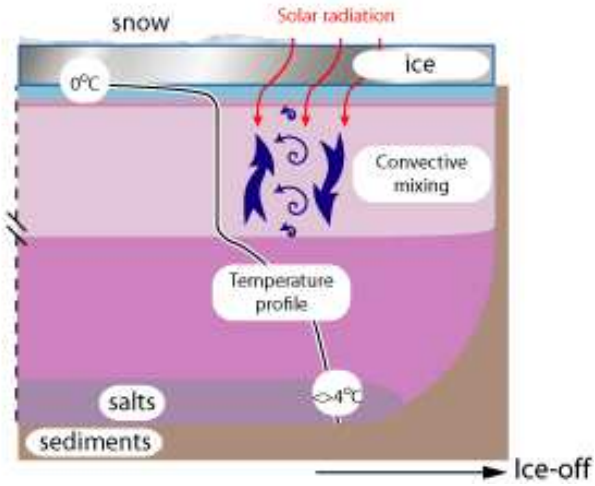

Figure 1. Schematic of the vertical temperature distribution and external forcing during the convection development under ice.

Although convectively mixed temperature profiles have been reported in many ice-covered lakes, direct measurements of the mixing by convection under ice are extremely rare. One reason for that is the technical difficulty of performing measurements from the unreliable ice surface during the melting period, when convection is most intense. Another obstacle is the non-local structure of convective mixing, which takes form of quasi-organized vertical water motions—convective cells or 'plumes'—with irregular distribution of velocities and temperatures across them. Little is known about spatial structure of radiatively-driven convection, test experiments with large eddy simulations model (Mironov et al. 2001) suggest the convective cells have lateral dimensions of several meters (Fig. 2a). Another indirect evidence of the coherent lateral structure of convection under ice is the typical melting pattern observed sometimes on the ice surface during melting (Fig. 2b). Although other processes, such as pumping of the lake water over the ice surface by the snow pressure, may contribute to formation of the observed patterns (Tsai und Wettlaufer 2007), their probable connection to the convection under ice has been discussed by a number of researchers (Brunt 1946; Woodcock 1965; Katsaros 1981).

The spatial heterogeneity of convection makes troublesome application of point measurement methods, like acoustic Doppler velocimetry, usually applied in turbulent environments. An appropriate vertical resolution may be achieved with the help of free-falling (free-rising) profilers supplied with sensors resolving the vertical fine structure of the convective layer. An attempt of convection measurements in ice-covered Lake Vendyurskoe (Russia) was reported by Jonas et al. (2003). The authors obtained 11 profiles of temperature microstructure and estimated the dissipation rate of convective energy by fitting the Batchelor-type model temperature spectrum to the measured temperature fluctuations spectra. Estimation of the dissipation rate from temperature microstructure is somewhat ambiguous, since Batchelor spectrum fitting involves two unknown parameters, the kinetic energy dissipation rate and the dissipation of the temperature variance (Oakey 1982). An alternative method consists in measuring the fine structure of the velocity shear, whose spectrum is known to scale well with the dissipation rate as the empirical Nasmyth spectrum (Nasmyth 1970).

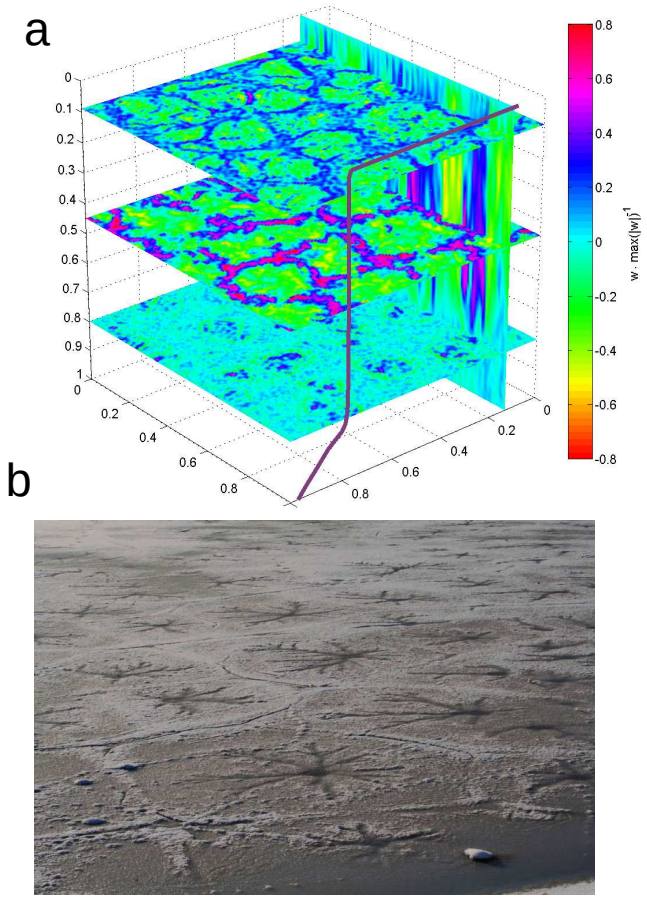

Figure 2. (a) Vertical velocities in the convectively mixed layer under ice as provided by large eddy simulations (Mironov et al. 2001). Velocities are made dimensionless by dividing through the maximum absolute value. Coordinates are scaled with the corresponding domain sizes. The solid line in the foreground is the dimensionless temperature profile. One vertical slice and three horizontal slices are shown corresponding to the top (0.1), middle (0.45) and bottom (0.8) of the convectively mixed layer. (b) Cell patterns on the ice surface of a small pond "Kleiner Kiel" (Kiel, Germany) in winter 2010 (Picture courtesy of Marcus Seeger).

In order to estimate the energetic constituents of convection under ice and range of its variability due to variations in the solar radiation we performed a field experiment in Finnish Lake Pääjärvi during the melting season 2011. Profiles of shear microstructure were taken continuously during 2 weeks at 1-2 hour intervals and were complemented by registrations of lake temperature and under-ice radiation. The study covered the last phase of the ice-covered period, with the last measurements performed during ice break-up. By this, the convection characteristics were captured at their most energetic stage. First results of the experiment are presented below.

2. Lake Pääjärvi and Measurements Setup

Pääjärvi is located at 61º04'N, 25º08'E (Fig. 3). The lake has the mean and maximum depths of 15 m and 87 m respectively, its surface area is 13.4 km^2. The average freezing and melting dates are by 30 November and 05 May respectively (Kärkäs 2000).

In winter 2010-2011 five thermistor chains were installed in the lake, 4 in proximity of the shallow West, South, East and North shorelines and a single, deep point near the lake centre. All chains were composed of RBR Canada loggers (accuracy ± 0.002°C) and were all configured at recording frequencies of 0.1 Hz. A weather platform was installed in the western part of the lake equipped with meteorological loggers and, additionally, with a PAR sensor located under the ice surface. The shear microstructure (MSS) profiler MSS-60 (ISW Wassermesstechnik) was installed in the western bay at the distance 300 m from the lake shore and was equipped with two airfoil velocity shear sensors for estimation of dissipation rate of the turbulence kinetic energy (ε), and a fast response thermistor for estimation of temperature and density fields. The profiler was operated from the lake shore, through an ice hole maintained artificially throughout the winter. The instrument was allowed to rise through the water column at a speed of 0.4 m s^{-1} taking measurements at 1024 Hz. 100 profiles were taken between 14 and 24 April, with the minimum interval between profiles of 60 min to avoid previous mixing produced by the profiler itself.

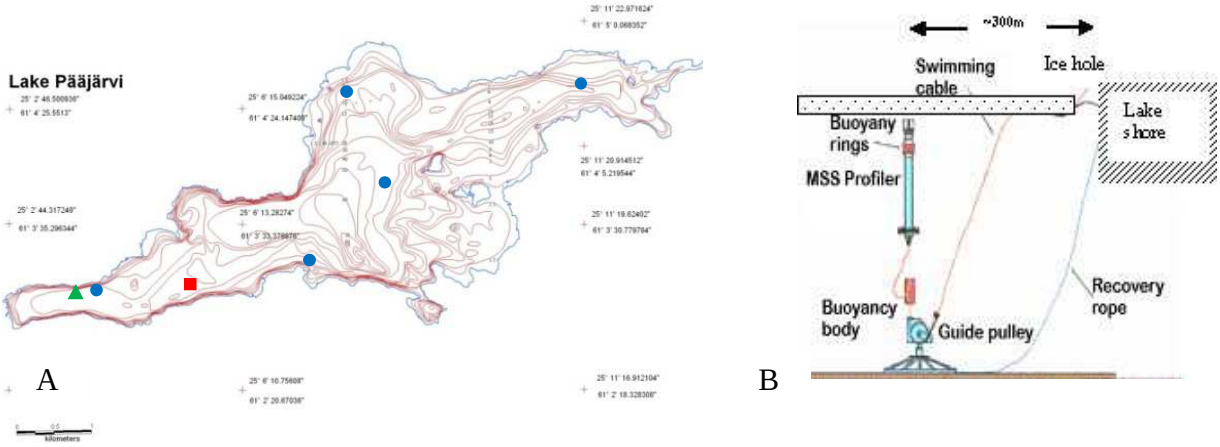

Figure 3. (a) Lake Pääjärvi bathymetric map with locations of the microstructure profiler (green triangle), weather platform with radiation sensors (red square) and thermistor chains (blue circles); (b) Schematic of the microstructure measurements setup.

The lower 0-1.0 m was excluded because the sinking velocity of the profiler was not constant. Subsequently, the dissipation rate ε was calculated from the measured velocity shear $\partial U/\partial z$ according to (Hinze 1959):

$$\varepsilon = \frac{15}{2}\nu\overline{\left(\frac{\partial u}{\partial z}\right)^2} \ [\mathrm{m^2 \cdot s^{-3}}] \qquad \textbf{[1]}$$

where ν [$m^2 \cdot s^{-1}$] is the kinematic viscosity of water, u refers to the turbulent velocity fluctuations. Correction for the part of the velocity fluctuations spectra not resolved by the shear probe was done by iterative fitting to the quasi-universal Nasmyth spectrum (Moum u. a. 1995).

3. Background Temperature and Under-ice Radiation Conditions in Spring 2011

The snow cover of 20-40 cm on the lake surface prevented fast ice growth in winter preceding the field study. The snow quickly melted in the first half of April 2011 due to sunny weather, and a large amount of radiation penetrated through relatively thin (~30cm) ice cover into the weakly stratified water column (Fig. 4).

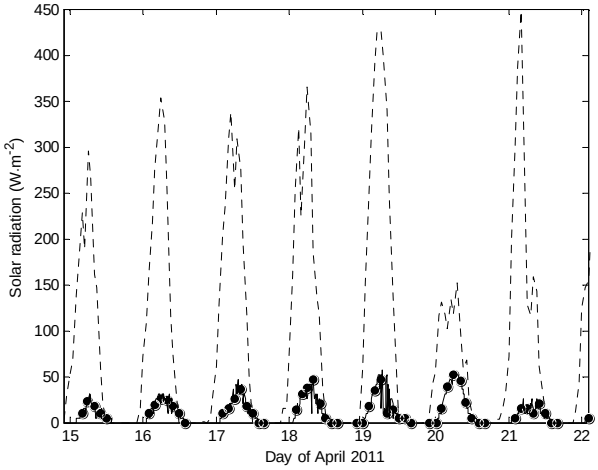

Figure 4. Downward solar radiation flux at the lake surface (dashed line) and under the ice cover (solid line).

As a result, the convectively mixed layer quickly advanced at the rate of more than 3 mday^{-1} (cf. temperature profiles taken in the central part of the lake in Fig. 5A). To the starting moment of microstructure profiling on 14 April the measurements site of 10 m depth was completely mixed to the bottom, except a thin layer, where mixing was prevented by a higher salinity (Fig. 5B). From that time on, convection distributed radiative heating across the entire water column resulting in graduate warming of the water column.

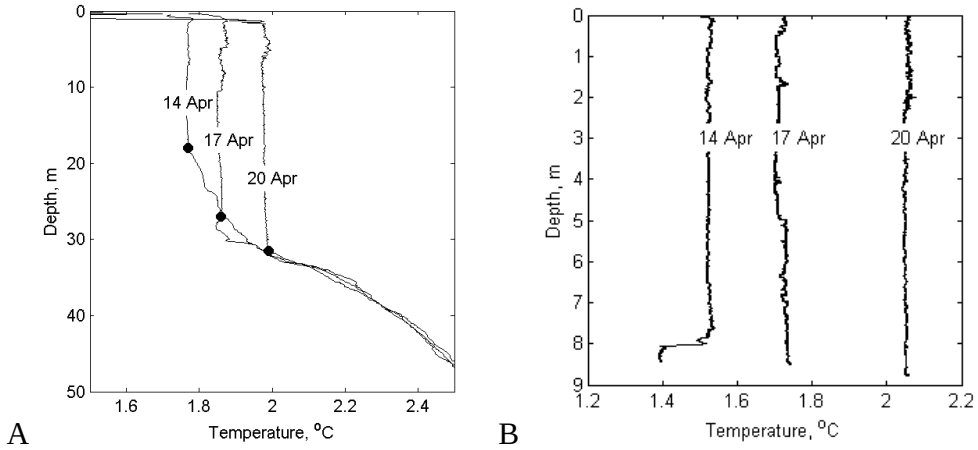

Figure 5. Convective temperature profiles (a) in the central part of Lake Pääjärvi and (b) at the microstructure measurements site, spring 2011. Dots in panel A mark the approximate bottom of the convectively mixed layer.

4. Dissipation Rates Estimated from the Microstructure Profiles

Estimations of dissipation rates suggest appreciable mixing produced by convection: depth-averaged values are about 10^{-8} Wkg^{-1} that is about 2 orders of magnitude higher than the background values of 10^{-10} Wkg^{-1} typically registered in the lake interior away from the boundary layers.

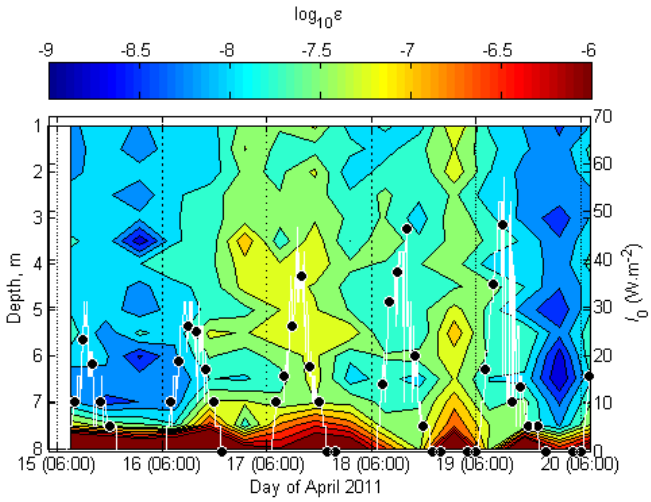

Figure 6. Time-depth diagram of the dissipation rate. The inder-ice radiation level during the same period is shown as white line for reference.

The dissipation rates reveal appreciable temporal variability, whose relation to the diurnal cycle of radiation under ice is not evident (Fig. 6). Remarkably high dissipation rates of up to 10^{-6} W kg^{-1} were registered in the lower part of the water column suggesting strong bottom boundary mixing. A probable reason for these currents may be elucidated from the lateral temperature differences between the near-shore areas and the central part of the lake (Fig. 5): At the beginning of the convective period, on 14 April, the mixed layer in deep central part of the lake is about 0.2°C warmer than the near-shore area; in turn, on 20 April the central part of the lake is 0.1°C colder than the litoral zone. Apparently, several factors contribute to this differential heating, such as differences in the amount of the radiation penetrating the ice (at the earlier stage, of convection the central part of the lake was snow-free, but snow cover still resided near the lake shores) and variations in the lake depth, which affect the amount of heat stored in the water column. On the lake-wide scale, Lateral temperature differences of 0.1-0.2°C are able to produce density-driven circulation with corresponding shear mixing at the lake bottom (see Rizk et al. 2012, *this volume*).

The diurnal cycle in the convective mixing becomes evident in the dissipation rate profiles averaged over 4-hour bins and then over the entire measurement period (Fig. 7): The dissipation rates vary during a day within an order of magnitude, the minimum rates are observed right before the sunrise at about 6:00 and the maximum ones are from the late afternoon right before the sunset (18:00).

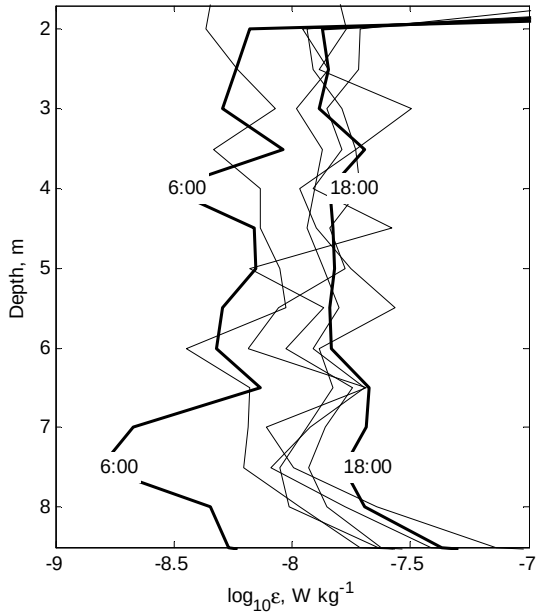

Figure 7. Vertical profiles of dissipation rates at different times of day averaged over the entire measurements period. The offset between profiles is 4 hours. Thick lines show the profiles before the sunrise (6:00 local time) and before the sunset (18:00 local time).

5. Convective Energy Budget

For the horizontally homogeneous shear-free convective layer, the budget equation for the turbulence kinetic energy integrated over the mixed layer depth reads,

$$\frac{d}{dt}\left(\int_0^h e dz\right) = -\int_0^h B dz - F_h - \int_0^h \varepsilon dz\,, \qquad \textbf{[2]}$$

where e is the convective energy, ε is its dissipation rate, B is the energy production by buoyancy forces, F_h is the vertical flux of energy at the bottom of the mixed layer. To arrive at Eq. (2), z axis has been directed downwards with origin at the top of the convective layer, use has been made of boundary conditions $e = 0$ at $z = 0$ and $z = h$, and the energy flux at $z = 0$ has been neglected. Two cases are particularly relevant to the diurnal cycle of convection. The first one is convection developing at the background of neutral stratification (this case corresponds to the early stage of diurnal convection right after the sunrise). Then, the energy budget (2) is reduced to

$$\frac{d}{dt}\left(\int_\delta^h e dz\right) = -\int_\delta^h B dz - \int_\delta^h \varepsilon dz\,. \qquad \textbf{[3]}$$

The second situation corresponds to convection occupying the entire water column, $h = D$, where D is the depth. The energy budget is given by the simple balance between production and dissipation:

$$\int_{\delta}^{h} B dz = \int_{\delta}^{h} \varepsilon dz \qquad \textbf{[4]}$$

The energy production rate B, can be found from the heat transport equation in one-dimensional form

$$\alpha g \frac{\partial T}{\partial t} = -\frac{\partial B}{\partial z} - \alpha g \frac{\partial I}{\partial z}, \qquad \textbf{[5]}$$

where α is the thermal expansion coefficient, g is the acceleration due to gravity, T is the temperature and I is the radiation flux. Assuming a homogeneous vertical temperature distribution over the convective layer, the bulk production rate B in the layer of thickness h is found as

$$\int_{0}^{h} B\,dz = \alpha g \left(\frac{I(0) + I(h)}{2} - \frac{1}{h} \int_{0}^{h} I(z)\,dz \right). \qquad \textbf{[6]}$$

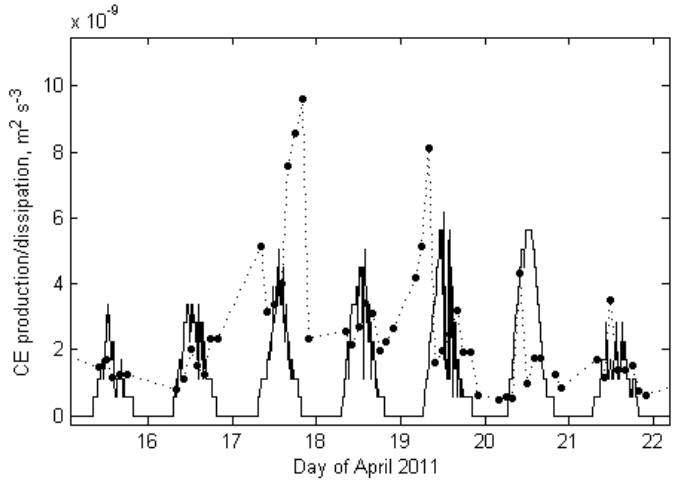

Figure 8. time series of production (solid line, Eq. 6) and dissipation (dashed line) of the convective kinetic energy averaged over the water column.

We approximated the vertical distribution of solar radiation within the water column by an exponential decay function with extinction coefficient of 2 m^{-1}, characteristic of Lake Pääjärvi, and substituted the resulting radiation flux into Eq. 6 for estimation of the convective energy production. When compared with the dissipation rates, the daytime cycle of the production rates is followed by the dissipation rates fairy well (Fig. 8). That is, the production-dissipation balance (Eq. 4) is satisfied. However, the nighttime dissipation rates are sometimes remarkable and even exceed the daytime values. This fact suggests an additional mechanism of the mixing generation besides the radiation-driven convection. As mentioned above, bottom boundary mixing produced

by the density currents is a feasible explanation for high dissipation rates in the absence of convection.

6. Conclusions

We have presented the first comprehensive dataset on the mixing rates produced by radiation penetrating the ice. Mean dissipation rates, as recovered from the shear microstructure, group around 10^{-8} W kg^{-1} and vary within an order of magnitude in the diurnal cycle. The production-dissipation balance holds true during the daytime convection. The data suggest significant mixing during the nighttime, when no convection takes place. Mixing is concentrated in the bottom boundary layer that indicates its generation by the bottom shear. A feasible reason for the shear mixing production is the density circulation driven by laterally inhomogeneous radiative heating between shallow and deep regions of the lake.

Acknowledgments

We thank Christof Engelhardt (Leibniz-Institute of Freshwater Ecology and Inland Fisheries, Berlin) for his valuable help in designing, organizing and performing the field study. The study would not be possible without the much appreciated support of the Lammi Biological Station staff. Dmitri Mironov (German Weather Service) has kindly provided us with an example dataset from large eddy simulations of convection under ice. We thank Hartmut Prandke (ISW Wassermesstechnik) for the consultative help and fruitful discussions on interpretation of microstructure data. This study is part of the research project KI-853-5/1 funded by the German Research Foundation (DFG).

References

Bengtsson, L., 1986. Dispersion in ice-covered lakes. Nordic hydrology, 17, 151–170.

Brunt, D., 1946. Patterns in ice and cloud. Weather, 1, 184–185.

Farmer, D. M., 1975. Penetrative convection in the absence of mean shear. Quarterly Journal of the Royal Meteorological Society, 101, 869–891.

Hinze, J., 1959. Turbulence. MeGraw Hill Book, NY, 586 pp.

Hobbie, J., 1973. Arctic limnology: a review. Alaskan Arctic Tundra. Arctic Institute of North America Technical Paper 25, 127–168.

Jewson, D., Granin, N., Zhdanov, A., and Gnatovsky, R., 2009. Effect of snow depth on under-ice irradiance and growth of Aulacoseira baicalensis in Lake Baikal. Aquatic Ecology, 43, 673–679.

Jonas, T., Terzhevik, A. Y., Mironov, D. V., and Wüest, A., 2003. Radiatively driven convection in an ice-covered lake investigated by using temperature microstructure technique. Journal of Geophysical Research, 108, 3183, doi:10.1029/2002JC001316.

Kärkäs, E., 2000. The ice season of Lake Pääjärvi in southern Finland. Geophysica, 36, 69–84.

Katsaros, K. B., 1981. Convection patterns in a pond. Bulletin of the American Meteorological Society,62, 1446–1453.

Matthews, P., and Heaney, S., 1987. Solar heating and its influence on mixing in ice-covered lakes. Freshwater Biology, 18, 135–149.

Mironov, D. V., Danilov S., and Olbers D., 2001. Large-eddy simulation of radiatively-driven convection in ice-covered lakes. Proc. of the 6th Workshop on Physical Processes in Natural Waters, X.Casamitjana (Ed.), 71–75, University of Girona, Girona, Spain.

Mironov, D., Terzhevik, A., Kirillin, G., Jonas, T., Malm, J., and Farmer, D., 2002. Radiatively driven convection in ice-covered lakes: Observations, scaling, and a mixed layer model. Journal Of Geophysical Research-Oceans,107, doi:10.1029/2001JC000892

Moum, J., M. Gregg, R. Lien, and M. Carr., 1995. Comparison of turbulence kinetic energy dissipation rate estimates from two ocean microstructure profilers. Journal of Atmospheric and Oceanic Technology, 12, 346.

Nasmyth, P. W., 1970. Oceanic turbulence. PhD Thesis, Univ. of British Columbia.

Oakey, N., 1982. Determination of the rate of dissipation of turbulent energy from simultaneous temperature and velocity shear microstructure measurements. Journal of Physical Oceanography, 12, 256–271.

Tsai, V. C., and Wettlaufer, J. S., 2007. Star patterns on lake ice. Physical Review E 75, 066105, doi:10.1103/PhysRevE.75.066105

Woodcock, A. H., 1965. Melt patterns in ice over shallow waters. Limnology and Oceanography, 10, 290–297.